

Orbital Selectivity and Magnetic Ordering in Fe intercalated Dirac Semimetal Bi_2Se_3

S. Koley^{1*} and Saurabh Basu²

¹ *Department of Physics, North Eastern Hill University, Shillong, Meghalaya, 793022 India and*

² *Department of Physics, Indian Institute of Technology Guwahati, Assam, 781039 India*

In this paper we investigate the intercalation effects of Iron (Fe) in the van der Waals gap of Bi_2Se_3 on the magnetic and transport properties using first-principles band structure estimations combined with dynamical mean-field theory. The Dirac cone in the band structure of parent Bismuth Selenide is modified via Fe intercalation at moderate densities. Further inclusion of electronic correlations found to result in the emergence of novel and exotic properties in an intercalated Bi_2Se_3 . Accompanied by unconventional structural effects, the onset of an orbital selective metal insulator transition in the Fe $3d$ orbitals brings about a magnetic phase transition in the Fe intercalated Bi_2Se_3 . Additionally we have explored the dependency of the electron-electron correlations on the magnetic ordering and the effects of intercalation in establishing new physical properties.

PACS numbers: 71.10.Hf, 63.20.dk, 74.25.Jb

I. INTRODUCTION

Topological insulators (TI) denote materials with properties dominated by the bulk insulating states, while their surface electronic structures are found to be metallic in nature¹⁻⁴. In these TIs, if spin-orbit coupling (SOC) exceeds the band gap and induce a band inversion, a Dirac type band structure emerges, and subsequently, the conducting states appear at the surfaces as demanded by the time-reversal symmetry. In recent times, these topological surface states are engineered in numerous ways to inspect their exotic properties and applicability⁵. Specifically, intercalation and doping by the transition metals (TM) in topological insulators and breaking of the time reversal symmetry are new features that are gathering interest in recent times. In addition, several exciting phenomena such as, the realization of quantum anomalous Hall effect^{6,7} etc. are likely to be possible.

Intercalation by foreign materials into the layered topological insulators changes properties of the parent compounds and possesses versatile applications, such as in superconductors, ambipolar transistors, quantum computers, battery electrodes and solid lubricants⁸. In particular, intercalation by the transition metals are expected to modify the time reversal symmetry induced band inversion and change the linearly dispersing bands by the reformed topological surface states. A well-known three dimensional topological insulator is Bi_2Se_3 ⁹ with a 0.3 eV gap in its bulk, alongwith the presence of a Dirac cone in the $K - \Gamma - M$ direction. Ab initio electronic structure calculations¹⁰ and electron scattering experiments have convincingly demonstrated topological properties of Bi_2Se_3 . Further, doped Bi_2Se_3 is currently being investigated due to the prospects of observing a new phenomenon that occurs when the topological surface states interact with different type of impurities or with other electronic states in the bulk. Intercalating Bismuth Selenide with Cu to get superconductivity below 4K was a potential discovery¹¹. Since it is a layered material, there is a van der Waals gap (gap between two consecutive layers of the material and the layers have van der

Waals interaction between them) in the crystal structure, making it favourable for intercalation with other materials as well, such as, Fe, Sr, Ag and many others. Intercalation into host materials with these has the prospects of achieving new energy storage materials.

The present paper focuses on the intercalation of topological insulating compound Bi_2Se_3 with Fe. The percentage of intercalation in these layered materials is determined by the physical size of the inserted material, structural stability and energetically favourable state of the host after insertion. Most of the time, the intercalation is governed by the likelihood of the host to retain its charge neutrality¹². Intercalation with small alkali metals, such as, Li etc. is relatively easy due to the size, while the ionic nature of the intercalant determines the probability of success of the intercalation in most cases. With all these issues in mind, intercalation with a zerovalent material is of a greater advantage, since it does not change the oxidation state of the host material, which, as a result, allows the insertion of a lot of zerovalent materials (e.g., Au, Ag, Fe, Cu and Ni) in the topological insulators¹². It does not affect the layered host Bi_2Se_3 , thus enabling an accurate intercalation. Here we used nearly 10 atomic percent of zerovalent Fe into layered Bi_2Se_3 crystals. Earlier studies have observed that Fe-doped Bi_2Se_3 is dominated by ferromagnetic interactions¹³. It is relevant to mention here that magnetism can also be achieved by Cr doping, where onset of antiferromagnetic correlations was observed¹⁴. Further quantum anomalous Hall state was also discovered in vanadium doped topologically insulating films¹⁵, which makes magnetic topological insulators as candidates for electronic applications. The discovery of the magnetic topological insulators has become interesting with an appearance of integer moments which may be related to half-metallic behaviour¹⁶.

Parent Bi_2Se_3 , when doped with TM, such as, Cr and Fe, shows an insulating behaviour with reduced band gaps due to the hybridization between the d orbitals of the TM with the Se- p orbitals¹⁰. Interestingly, in the TI systems, strong spin-orbit coupling results in different

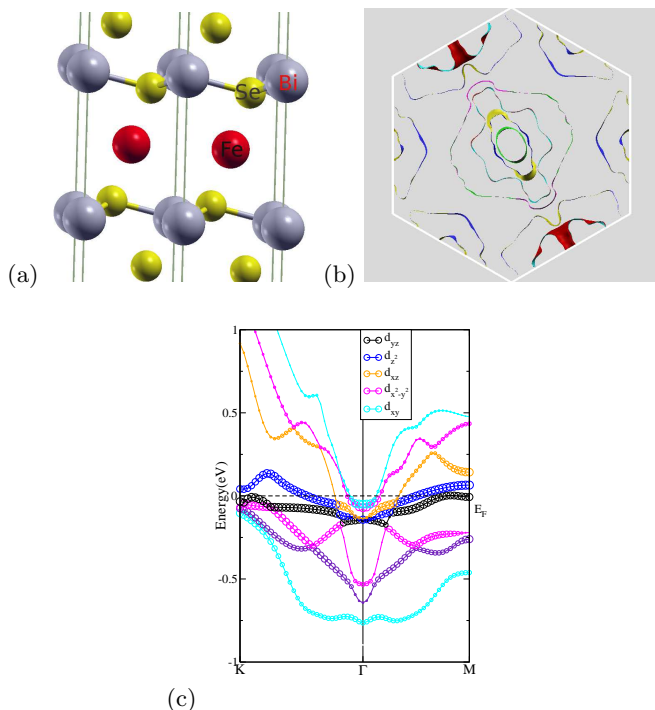


FIG. 1. (Color Online) (a) The crystal structure is shown where the atoms are labelled, (b) Fermi surface and (c) band structure of Fe intercalated Bi_2Se_3 . The Fermi surface reveals impurity d bands crossing the Fermi level. The high intensity region is for electrons, while the low intensity stands for holes. Intercalation results in disappearance of the band inversion at the Γ point and results in increase in the number of conduction electrons.

parity valance, and the conduction bands cross, thereby opening up a band gap to produce an inverted band structure. However in an intercalated Bi_2Se_3 , the TM atoms cause disorder which often induce some impurity bands in the band gap, leading to a number of versatile properties, including, in some cases, the strength of the spin-orbit coupling is reduced. It is well known that the $3d$ electrons in TM atoms contribute to magnetism with a maximum of five unpaired electrons. These $3d$ electrons may easily hybridize with the surrounding TI atoms, thereby reducing their average moments. For these reasons, several experimental explorations have emerged on magnetically doped TIs¹⁷. However on the theoretical front, research on Fe intercalation in Bi_2Se_3 is still lacking. Therefore, there is a strong motivation for us to study the effects of Fe intercalation on structural and electronic properties of Bi_2Se_3 .

II. DFT+DMFT

In this paper we use first-principles spin-polarized density functional theory (DFT) calculations combined with embedded dynamical mean field theory to demonstrate the intercalation induced changes in the elec-

tronic properties of Bi_2Se_3 using Fe as intercalant. First principles structure calculations were performed using WIEN2k full-potential linearized augmented plane wave (FP-LAPW) ab initio package¹⁸ within the DFT¹⁹ formalism to get the band structure and the density of states (DOS). A generalized gradient approximation Perdew-Burke-Ernzerhof (GGA-PBE) exchange correlation potential is used here. The relativistic effects and the spin-orbit coupling have been included in the DFT calculation. In fact, for realization of the Dirac cone at the Γ point in the parent Bi_2Se_3 crucially depends on the spin-orbit coupling. The muffin-tin radii, R_{MT} are chosen as 2.4 a.u. for Bi, 2.1 a.u. for Se and 2.3 a.u. for Fe atoms. The parameter, Rk_{max} (Rk_{max} stands for the product of the smallest atomic sphere radius R_{MT} times the largest k -vector k_{max}) is chosen to be 7.0 and 1000 k -points with a $10 \times 10 \times 10$ k -mesh is employed here for structural optimization. A 2×2 supercell is used for the intercalation of Fe. Intercalation is produced via introduction of the atoms into the interlayer space. The length of Fe-Fe bond in a layer is 0.45 nm while the length of Fe-Se bond along c direction becomes 0.285 nm after intercalation. Further, for the total energy calculations, all atoms are relaxed until the maximum force is smaller than $0.01 \text{ eV}/\text{\AA}$. Finally the self consistent field (scf) calculations are performed till an energy accuracy of 0.0001 eV is reached. The lattice constants obtained from our calculation agrees nicely with the previous experiment¹². Then the band structure and the atom-resolved density of states are calculated from the converged scf calculations (see Fig.1 and Fig.2).

The spectral function shows partially occupied Se- $4p$, Bi- $6p$ and Fe- $3d$ bands near the Fermi level for the Fe-intercalated sample. The energy bandgap in parent Bi_2Se_3 is about 0.3 eV (in good accord with the reported experiments and theory) closes with Fe-intercalation and impurity bands dominate near the Fermi level (see Fig.1c and Fig.2). For performing correlated electronic structure and spectra calculations, a fully charge-self-consistent dynamical mean field theory (DMFT) is employed via the EDMFTF package²⁰, which implements a combined DFT and DMFT derived from the stationary Luttinger-Ward functional. Here, the exact double-counting of DFT and DMFT and Coulomb interaction are well treated and the Green's function is determined self-consistently. In strongly correlated systems, DFT+DMFT has been successful in detailing a lot of important results^{21–26}. In the DMFT section, the non-interacting Hamiltonian is added with the Coulomb interaction term, H_{int} ²⁷, to incorporate the effects of correlated Fe- $3d$ orbitals and also a self energy functional, Σ_{dc} to take care of the double counting. The total Hamiltonian, except the Σ_{dc} term is expressed as,

$$H = \sum_{k,a,\sigma} \epsilon_{k,a} c_{k,a,\sigma}^\dagger c_{k,a,\sigma} + U \sum_{i,a} n_{i a \uparrow} n_{i a \downarrow} +$$

$$U' \sum_{i,a,b,\sigma,\sigma'} n_{ia\sigma} n_{ib\sigma'} - J_H \sum_{i,a,b} S_{ia} \cdot S_{ib} \quad (1)$$

where $\epsilon_{k,a}$ is the band dispersion which includes the effects of SOC, σ stands for up and down spins and U and U' are the intra- and inter-orbital Coulomb interaction terms between electrons with opposite spins in the same orbital and between electrons with parallel spins in different orbitals respectively, and J_H is the Hund's coupling. The inter-orbital term (U') is reduced by the ferromagnetic coupling due to Hund's first rule that favors the alignment of spins. We also have a relationship between different energy scales, namely, U , U' and J_H given by, $U' = U - 2J_H$. In our work we have considered $J_H=1.25$ eV (reasonable for Fe-3d bands) and varied U over a realistic range.

Finally the total Hamiltonian is solved using the DMFT method. The correlated five Fe-3d orbitals are treated dynamically within the DMFT based on orbital projection-embedding scheme accomplished via the EDMFT package, while the Bi and Se- p orbitals are treated at the DFT level. The impurity solver used in the DMFT code is the continuous time quantum Monte Carlo (CT-QMC) in the hybridization expansion method²⁸. The parameters, namely, the Coulomb interaction U , Hund's coupling, (J_H) and the inverse temperature, β ($= 1/k_B T$) are varied within an experimentally realizable range to get T and U dependence of the intercalated system. The DFT+DMFT calculations are converged upto precision of 0.0001 with respect to the charge density, the chemical potential and the self energy with considering step over E as 10^{-6} . Finally the maximum entropy method²⁹ is used for the analytical continuation of the self-energy from the imaginary axis to real frequencies with an auxiliary Green's function. Then from the real frequency Green's function, the momentum-resolved spectral functions and the density of states are obtained. To check the stability and accuracy of the result we have used Padé approximation in addition to the maximum entropy method used in the EDMFTF package.

III. RESULTS AND DISCUSSION

We have considered Fe intercalation in between two quintuple layers of Bi_2Se_3 , a situation that is energetically more favorable. In each of the quintuple layer, the hexagonal atomic planes are arranged following the sequence of Se1-Bi-Se2-Bi-Se1 along the z -direction with covalent bonding between the atoms, and the Se1 and Se2 atoms stand for two inequivalent Selenium atoms. So the intercalated Fe atom will be in the environment of a Se1 atom. First we study the change in the band structure of Bi_2Se_3 due to the intercalation by Fe (see Fig.1c).

The validity of the EDMFT package is well established^{21,22}. Moreover our calculated results, such as the momentum resolved spectral function and the magnetic order are consistent with the earlier iron doped

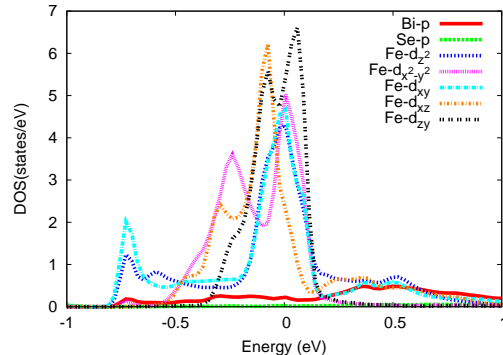


FIG. 2. (Color Online) Spectral function of Fe intercalated Bi_2Se_3 . For the effective model incorporating conduction electrons within DMFT calculations, we use the Bi- p , Se- p and Fe-3d bands crossing Fermi Energy ($E_F=0$), while Bi- p and Se- p bands have very less spectral weights at the Fermi energy, the Fe- d bands dominate the low energy physics.

Bi_2Se_3 results¹⁴. We also present DMFT one particle spectrum for Cu intercalated Bi_2Se_3 which shows good agreement with the earlier experiments³⁰ (zero energy peak in the density of states). Since a Fe-based system consists of unfilled 3d-orbitals and possesses different values of the Coulomb interaction, we varied it within a reasonable range, and determined the final values of U and J_H for the system (considering earlier experimental results), which are found as 5.5 eV and 1.25 eV respectively. Large values of U , that is, strong electronic correlations renormalize the spectral function considerably. The total density of states of an intercalated Bi_2Se_3 is presented in Fig.3 for different values of U . In comparison with the DFT DOS, the correlated electronic spectra from the DMFT are very distinct, indicating that this system is a correlated bad metal. It is observed that, the spectral weight at the Fermi level, E_F reduces with increasing U . The Fe intercalation leads to an abrupt change of the electronic structure and the 3d orbitals of the Fe atom dominate the low-energy properties of the compound (Fig.2). This is in contrast with Fe-doped Bi_2Se_3 which shows an insulating behaviour, and instead here we get bad metal. Further, we obtain the temperature dependence of the DOS, by employing a different value of β in the EDMFTF. This yields that with decreasing temperature, the total spectral weight of the d -orbital DOS increases at the Fermi level, while at around 50 K, the d_{z^2} and $d_{x^2-y^2}$ orbitals undergo an orbital selective metal-insulator transition as shown in Fig.4a. The orbital selectivity is confirmed from the divergence of $\text{Im}\Sigma(\omega)$ at the Fermi level for the d_{z^2} and $d_{x^2-y^2}$ orbitals, while the other orbitals provide support for metallic features at low energies. This orbital selectivity at 50K can be related to the onset of a possible magnetic order, as also corroborated by the magnetic susceptibility plot (Fig.4b). The right inset of Fig.4a shows $\text{Im}\Sigma(\omega)$ at 100 K which reveals non-Fermi liquid features due to high T , while the left inset of Fig.4a depicts the resistiv-

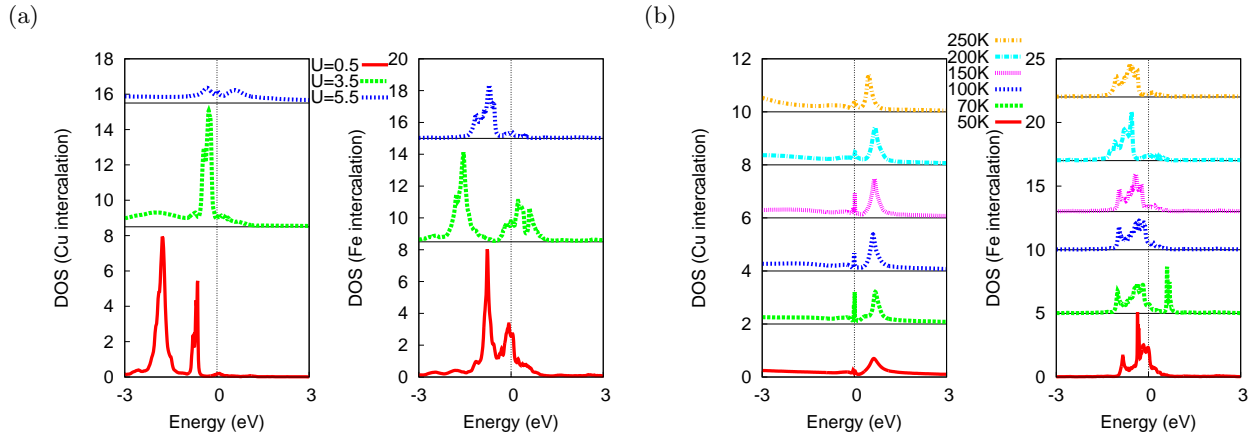


FIG. 3. (Color Online) Total density of states from DFT+DMFT for Cu and Fe intercalated Bi_2Se_3 at (a) various values of U and (b) at different temperatures, T . DFT+DMFT density of states for Cu intercalation is provided to compare with the earlier results³⁰. Spectral density at E_F remains finite throughout the temperature range for Cu intercalation, whereas for the Fe-intercalated compound, it decreases with temperature and the system behaves as correlated bad metal. Density of states are shifted along the y -axis to reflect changes induced by Coulomb interaction and temperature respectively.

ity data at low temperatures, which shows proportionality to T with a change of slope around 50 K. Change of slope around 50 K in resistivity further confirms an ordering transition to occur. This ordering transition is also coherence restoring transition because resistivity decreases at lower T . The transport observation also goes hand in hand with our prediction of a paramagnetic to a ferromagnetic transition, while the paramagnetic order can be considered as fluctuation of magnetic moments at high T . The observation of orbital selectivity and related magnetic order in Fe-intercalated systems is not surprising and can be argued to have originated from moderate U' (U' being the inter-orbital Coulomb repulsion) which leads to a selective Mottness in the multi-band situation. Interestingly, stabilization of the magnetic order enhances selective Mott features at low temperatures as a zero energy pole emerges in the $\text{Im}\Sigma(\omega)$ (d_z^2 and $d_{x^2-y^2}$, along with small mass enhancement in $\text{Re}\Sigma(\omega)$ of three other d-orbitals.

Next we present angle resolved photoemission spectra of Fe intercalated Bi_2Se_3 in Fig.5a and Fig.5b. In contrast to the conventional DFT band structure results, it shows pronounced renormalized effects in the band structures owing to strong electronic correlations. The characteristic Dirac-like dispersion manifests above the Fermi level at the Γ point for both low (50 K) and high (200 K) temperatures. Near the Fermi level (FL), two bands cross the FL along the $K - \Gamma - M$ direction. Further at the lower temperature (that is, 50 K), the lower band sinks below the FL signaling a transition from a hole pocket to an electron pocket in the $\Gamma - K$ and $\Gamma - M$ directions. In comparison with the DFT band structure results, the DMFT momentum resolved spectra indicate a correlation driven Lifshitz transition. It may also be noted that in this study, the intercalation density is 10% (we have examined other (lower) densities, although not presented here), as this scenario seems to be ideal for observing

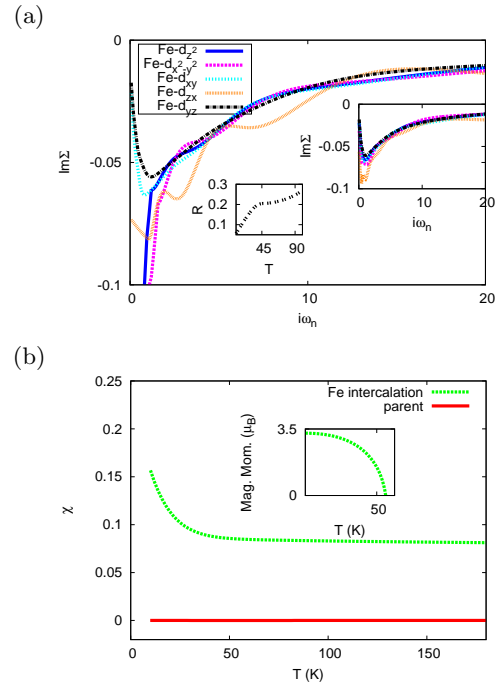


FIG. 4. (Color Online) (a) Orbital dependent self energies from DFT+DMFT for Fe intercalated Bi_2Se_3 at combination of U , U' (5.5 eV and 3.0 eV) and $T=50$ K and $T=100$ K (right inset Fig.4a). Left inset shows normalized resistivity with temperature. (b) T dependent DMFT susceptibility, χ for the parent and the intercalated Bi_2Se_3 . χ for the intercalated compound shows steep increase at around 50 K, while as shown in the inset, the magnetic moment, m vanishes around the same temperature.

a magnetic phase transition. Our results also indicate emergence of small electron pockets around these two directions (namely, $\Gamma - K$ and $\Gamma - M$), which is further confirmed by the DMFT Fermi surface (FS) results (see

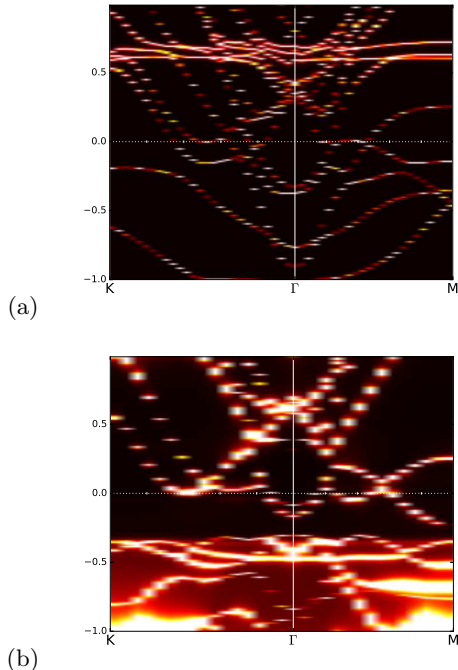


FIG. 5. (Color Online) Momentum resolved spectral function map for Fe intercalated Bi_2Se_3 at (i) low (50K) and (ii) high (200 K) temperatures.

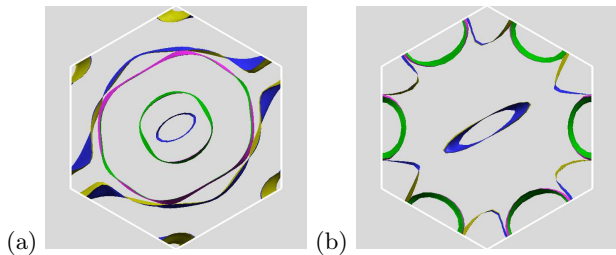


FIG. 6. (Color Online) Fermi surface map for Fe intercalated Bi_2Se_3 at (i) low (50K) and (ii) high (200 K) temperatures. Emergence of new pockets in the Brillouin zone edge is evident, whereas none of the electron pockets around the Γ point disappear.

Fig.6) discussed below.

Further to address intercalation dependent changes we calculate the DMFT FS at two different temperatures (namely, 50 K and 200 K). Combined with intercalation dependent evolution of the electronic structure, the Fermi surface map reveals connection between ordering and electronic correlations. Since the effect of electronic correlations is already described above, the DMFT FS deserves to be investigated. Both the DFT FS (Fig.1b) and the DMFT FS (Fig.6) are shown here for comparison. Both the results reveal presence of electron pockets around the Γ point and hole pockets around the K and the M points. In the DMFT results, with strong correlation being considered, the FS topology shows a sizeable change, that is, from five electron pockets, it becomes

three electron pockets at 50 K and finally a one electron pocket at 200 K around the Γ point. On the other hand, the hole pockets around the K and M points also undergo significant modification. We strongly believe that these modifications arise due to orbital dependent electronic structure reconstruction and essentially driving the system into a magnetically ordered phase.

To capture the nature of magnetic ordering by electronic correlations, we have calculated the temperature variation of the magnetic susceptibility and the moment from the EDMFT package. In Fig.4b we show the temperature dependence of the magnetic susceptibility, χ and the inset contains the variation of the magnetic moment, m with temperature. The parent compound Bi_2Se_3 possesses a weak diamagnetic character with almost no temperature dependence, while Fe intercalation makes the compound magnetic. The magnetic nature is confirmed to be ferromagnetic as χ shows a Curie behaviour with $\chi \sim (T - T_c)^{-1}$, with T_c as the Curie temperature. We have observed $T_c \sim 30\text{K}$. Moreover we have calculated the spin gap energy (denoted by the energy difference between the ferromagnetic and the weakly diamagnetic state), which reveals that the ferromagnetic state is more energetically stable. In Fe- Bi_2Se_3 system, the magnetic moments of Fe is about $3.5\mu_B$ and the other atoms have smaller magnetic moments (of about $0.001\text{-}0.01\mu_B$) which align antiparallely with the moments of the Fe atom. The system turns out to be magnetic with a value for the magnetic moment as $3.4\mu_B$. The spin up and spin down states are partially filled with a occupation difference between them resulting in a magnetic moment which is almost totally contributed by the Fe- $3d$ orbitals and the relevant electronic correlations.

In conclusion, the electronic correlations along with a reasonable spin-orbit coupling in Fe intercalated Bi_2Se_3 have been examined employing the DFT+DMFT method executed with the CT-QMC impurity solver. A strong correlation-driven electronic structure modification accompanied by a Lifshitz transition is found in the intercalated compound, indicating an ordered phase to set in at lower temperatures, which is significantly different than the parent compound. Both the electronic correlations and the spin-orbit coupling play major roles in the electronic structure and transport properties of intercalated compound. These generate tiny electron pockets around the $\Gamma - K$ and the $\Gamma - M$ directions. Our results are somewhat similar to the Fe-doped (not intercalated) Bi_2Se_3 compound, in the sense that it also shows different type of magnetic ordering with doping concentration and temperature¹³. All these results are new in literature and subject to further experimental study. The results mainly demonstrate many-body characteristics, such as many-body self-energy, spectral weight, presence of quasiparticles near the Fermi level, and a strong renormalization of the effective masses. Further explorations of the low temperature properties and other intercalation densities need to be undertaken in near future. Moreover increased T_c due to intercalation can lead to potential ap-

lications in the context of spintronic devices and energy storage materials^{32–35}. Our studies suggest that the Fe-intercalated Bi₂Se₃ could be an ideal system to identify the role of electronic correlations and spin-orbit coupling in magnetism of iron-based materials.

ACKNOWLEDGMENTS

This work is financially supported by DST women scientist grant SR/WOS-A/PM-80/2016(G). S. K. grate-

fully acknowledge Prof. M C Mahato for mentoring and useful conversations. SB acknowledges support from the SERB grant EMR/2015/001039.

-
- * sudiptakoley20@gmail.com
- ¹ C. L. Kane and E. J. Mele, *Phys. Rev. Lett.* **95**, 146802 (2005).
 - ² C. L. Kane and E. J. Mele, *Phys. Rev. Lett.* **95**, 226801 (2005).
 - ³ B. A. Bernevig, T. L. Hughes, and S.-C. Zhang, *Science* **314**, 1757 (2006).
 - ⁴ M. König *et al.*, *Science* **318**, 766 (2007).
 - ⁵ Guan Du *et al.*, *Nature Communications* **8**, 14466 (2017).
 - ⁶ R. Yu, *et al.*, *Science* **329**, 61 (2010).
 - ⁷ C.-Z. Chang, *et al.*, *Science* **340**, 167 (2013).
 - ⁸ T Wang *et al.*, *Adv Sci* **4**, 1600289 (2017).
 - ⁹ X.-L. Qi, and S.-C. Zhang, *Rev. Mod. Phys.* **83**, 1057 (2011); Y. Ando, *J. Phys. Soc. Jpn.* **82**, 102001 (2013).
 - ¹⁰ H. Zhang *et al.*, *Nat. Phys.* **5**, 438 (2009).
 - ¹¹ Y.S. Hor *et al.*, *Phys. Rev. Lett.* **104**, 057001 (2010).
 - ¹² K. J. Koski *et al.*, *J. Am. Chem. Soc.* **134**, 13773 (2012).
 - ¹³ Z.Salman *et al.*, *arXiv:1203.4850*.
 - ¹⁴ Y. H. Choi, *et al.*, *J. Appl. Phys.* **109**, 07E312 (2011).
 - ¹⁵ C.Z.Chang *et al.*, *Nat. Mater.* **14**, 473 (2015).
 - ¹⁶ P. Larson and Walter R. L. Lambrecht, *Phys. Rev. B* **78**, 195207 (2008).
 - ¹⁷ F. Zheng *et al.*, *Chalcogenide Letters* **14**, 551 (2017).
 - ¹⁸ P. Blaha, *et al.*, *WIEN2k, An Augmented Plane Wave + Local Orbitals Program for Calculating Crystal Properties* (Wien:Karlheinz Schwarz, Techn. Universitat Wien, 2001).
 - ¹⁹ T.L. Loucks, *Augmented Plane Wave Method* (New York:Benjamin, 1967); O.K. Andersen, *Solid State Commun.* **13**, 133 (1973); E. Wimmer, *et al.*, *Phys. Rev. B* **24**, 864 (1981).
 - ²⁰ K. Haule, C. Yee, and K. Kim, *Phys. Rev. B* **81**, 195107 (2010).
 - ²¹ K. kim *et al.*, *Nat. Mater.* **17**, 794 (2018).
 - ²² A. Eugene *et al.*, *Science* **359**, 186 (2018).
 - ²³ A. Taraphder, S. Koley, N.S. Vidhyadhiraja, and M.S. Laad, *Phys. Rev. Lett.*, **106**, 236405 (2011).
 - ²⁴ S. Koley, M.S. Laad, N.S. Vidhyadhiraja, and A. Taraphder, *Phys. Rev. B*, **90**, 115146 (2014).
 - ²⁵ A. Georges *et al.*, *Rev. Mod. Phys.* **68**, 13 (1996).
 - ²⁶ S. Koley, *Solid State Commun.* **251**, 23 (2017).
 - ²⁷ S. Koley, and S. Basu, *arXiv:1904.03698*.
 - ²⁸ K. Haule, *Phys. Rev. B* **75**, 155113 (2007).
 - ²⁹ M. Jarrell and J. E. Gubernatis, *Phys. Rep.* **269**, 133 (1996).
 - ³⁰ S. Sasaki *et al.*, *Phys. Rev. Lett.* **107**, 217001 (2011).
 - ³¹ T. Valla *et al.*, *Phys. Rev. Lett.* **108**, 117601 (2012).
 - ³² W. Müller-Warmuth, and R. Schöllhorn (Eds.) *Progress in Intercalation Research*, Kluwer: Dordrecht, The Netherlands, (1994); M. S. Dresselhaus, *Intercalation in Layered Materials*; NATOASI Series, Subseries B, Physics, Vol. 148; Plenum Press: New York, (1987); F. Levy *Intercalated Layered Materials* Reidel: Dordrecht, The Netherlands, (1979); M. S. Whittingham and A. J. Jacobson (Eds.) *Intercalation Chemistry* Academic Press: New York, (1982).
 - ³³ A.S. Aricò, P. Bruce, B. Scrosati, J.M. Tarascon, and W. V. Schalkwijk, *Nat. Mater.* **4**, 366 (2005).
 - ³⁴ M.S. Whittingham *J. Solid State Chem.* **29**, 303 (1979).
 - ³⁵ K. Kang, *et al.*, *Science* **311**, 977 (2006); J.M. Tarascon and M. Armand *Nature* **451**, 652 (2008).